Experimental study on the performance of the CFRP sheet-recycled aggregate concrete interface under dynamic loading conditions

Dong Li[1], Xinrui Wang[1], Jiangxing Zhang[1], Liu Jin[1*], Xiuli Du[1]

[1] Key Laboratory of Urban Security and Disaster Engineering of Ministry of Education, Beijing University of Technology, Beijing 100124, China
jinliu@bjut.edu.cn

Abstract. The combined application of Carbon Fiber Reinforced Polymer (CFRP) and recycled aggregate concrete is of great importance in conserving resources and reducing environmental pollution. A dynamic experimental study was conducted using a double-sided shear test method, and the bonding behavior of CFRP sheet-recycled aggregate concrete interface was analyzed. The effects of seven kinds of bond length, four kinds of bond width and three kinds of load rate on the interface properties were considered. The experimental results demonstrate that: 1) The main damage pattern of the CFRP sheet-recycled aggregate concrete interface is stripping damage of concrete surfaces. 2) As the bond length and bond width increase, the ultimate bearing capacity of the CFRP sheet-recycled aggregate concrete interface increases, and the influence of loading rate on the ultimate bearing capacity decreases. 3) It is evident that the interfacial fracture energy and interfacial shear stress are subject to a pronounced strain rate effect. In the bond-slip relationship of the interface, a reduction in bond width and an increase in loading rate result in an increase in the slip corresponding to the peak shear stress.

Keywords: CFRP sheet-concrete interaction; Recycled aggregate concrete; Loading rates; Ultimate bearing capacity

1 Introduction

In light of the ongoing acceleration of global urbanization and the concomitant expansion of the construction industry, reinforced concrete buildings have been experiencing ageing, demolition and renovation. More and more construction waste is generated in this process, causing serious pressure and impact on the resource environment. Repair and reinforcement of damaged structures and reuse of construction waste can effectively reduce construction waste. This has significant practical implications for the conservation of resources and the reduction of environmental pollution resulting from the disposal of waste concrete. [1].

W. Guo et al. (eds.), *Proceedings of the 3rd International Conference on Green Building, Civil Engineering and Smart City (GBCESC 2024)*, Advances in Engineering Research 264,
https://doi.org/10.2991/978-94-6463-728-1_29

In the field of structural engineering, Carbon Fiber Reinforced Polymer (CFRP) has been employed extensively for the reinforcement and repair of concrete building. It has the advantages of easy construction, good durability, high strength and light weight [2]. For end-of-life concrete, it can be broken, cleaned, graded, and mixed in a specific proportion to create recycled aggregate. The recycled aggregate will replace the natural aggregate in proportion to form recycled aggregate concrete, which can realize the reuse of resources [3]. Recycled aggregate concrete exhibits lower strength than normal aggregate concrete [4]. The use of CFRP sheets has been demonstrated to enhance the ductility and bearing capacity of recycled aggregate concrete beams [5]. The combined application of CFRP sheet and recycled aggregate concrete has become one of the current research hotspots in the field of concrete structure reinforcement and repair [6]. Under dynamic loading, the mechanical properties of CFRP-concrete interface differ significantly from those under static loading due to the strain rate effect. Currently, the dynamic bonding performance of CFRP sheet-recycled aggregate concrete interface is unclear. In this study, we carried out an in-depth study by experimental means and analyzed the damage pattern, ultimate bearing capacity, and interfacial fracture energy.

2 Experimental program

2.1 Experimental design and loading scheme

Fig. 1 shows the test device diagram of this paper, which adopts the form of double-sided shear test. The size of the concrete specimen is 300 mm × 100 mm × 100 mm. The specimens were installed and connected to a universal testing machine using a self-designed fixture. The CFRP sheet was applied symmetrically to both sides of the concrete specimen at the center axis. In order to prevent wedge damage at the load end of the concrete, a 50 mm non-bonded zone was set at the load end of the concrete. The distance from the lower edge of the non-bonding area to the fixture is 150 mm. The strain gauges are attached to the central axis of CFRP sheets on both sides. Because the strain gauge has a certain size, the same 30 mm spacing is used when the strain gauge is pasted. The initial strain gauge is bonded at 5 mm from the edge line of the unbonded area. During the test, the load sensor and the dynamic strain acquisition instrument automatically collect data.

2.2 Experimental materials

Concrete. In the tests, P.O 42.5 ordinary silicate cement was used for cement, medium-coarse river sand was used for fine aggregate, and tap water was used as mixed water. The replacement rate of recycled coarse aggregate was 100%, and the particle size was 5 - 20 mm continuous grading. According to the requirements of JGJ55-2011 [7], the mixing ratio of recycled aggregate concrete was designed. The proportion of constituents in concrete is as follows: water: cement: fine aggregate:

coarse aggregate = 1: 1.34: 2.65: 4.92. The 28-day cubic compressive strength of the concrete is 37.25 MPa, and the axial tensile strength is 3.36 MPa.

CFRP sheet. The fiber-reinforced composite used in this test was CFRP. CFRP sheets were produced by Carbon Engineering Co., Ltd. and tensile tests were conducted in accordance with the GB/T 3354-2014 standard [8]. The nominal thickness of the CFRP sheet was 0.167 mm. The measured tensile strength is 3861.9 MPa, the elastic modulus is 240 GPa, and the ultimate strain is 1.7 %.

Adhesive. The impregnating adhesive used in this test was the Carbone impregnating adhesive matched with the CFRP sheet. The tensile strength of the impregnated adhesive is 60.9 MPa, the elastic modulus is 3700 MPa, and the ultimate tensile strain is 2.0 %.

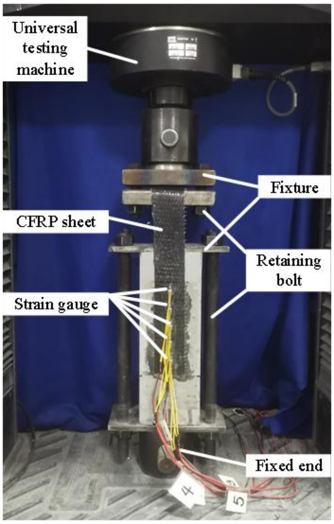

Fig. 1. Diagram of the test setup

2.3 Experimental protocol

The purpose of this test is to study the interfacial properties of CFRP sheet and recycled aggregate concrete under different loading rates. The test parameters include CFRP sheet bond length *L*, bond width *b* and loading rate *v*. The test scheme is shown in Table 1, where the loading rate is divided into 3 levels: S is quasi-static load, DⅠ~DⅡ are 2 levels of dynamic load. These loads correspond to the loading rates of 0.1 mm/min, 10 mm/min, and 100 mm/min, respectively. The strain rate for each load is 10^{-5}/s, 10^{-3}/s, and 10^{-2}/s. Taking into account the discreteness of the test results, each type contains three specimens. The remaining parameters in the specimen numbers indicate the bond length and bond width of the same group.

Table 1. Main parameters of the specimen.

Specimen number	L(mm)	b(mm)	v(mm/min)	Strain rate (s^{-1})
S-40-50			0.1	10^{-5}
DⅠ-40-50	40		10	10^{-3}
DⅠⅠ-40-50			100	10^{-2}
S-60-50			0.1	10^{-5}
DⅠ-60-50	60		10	10^{-3}
DⅠⅠ-60-50			100	10^{-2}
S-80-50			0.1	10^{-5}
DⅠ-80-50	80		10	10^{-3}
DⅠⅠ-80-50			100	10^{-2}
S-100-50			0.1	10^{-5}
DⅠ-100-50	100	50	10	10^{-3}
DⅠⅠ-100-50			100	10^{-2}
S-120-50			0.1	10^{-5}
DⅠ-120-50	120		10	10^{-3}
DⅠⅠ-120-50			100	10^{-2}
S-160-50			0.1	10^{-5}
DⅠ-160-50	160		10	10^{-3}
DⅠⅠ-160-50			100	10^{-2}
S-200-50			0.1	10^{-5}
DⅠ-200-50			10	10^{-3}
DⅠⅠ-200-50			100	10^{-2}
S-200-25			0.1	10^{-5}
DⅠ-200-25		25	10	10^{-3}
DⅠⅠ-200-25	200		100	10^{-2}
S-200-75			0.1	10^{-5}
DⅠ-200-75		75	10	10^{-3}
DⅠⅠ-200-75			100	10^{-2}
S-200-100			0.1	10^{-5}
DⅠ-200-100		100	10	10^{-3}
DⅠⅠ-200-100			100	10^{-2}

3 Experimental results and discussion

3.1 Damage pattern

Fig. 2 illustrates the main damage patterns of the tests. Most of the specimens showed a stripping damage of the concrete surface underneath the CFRP sheet. This indicates that for recycled aggregate concrete, the CFRP sheet can effectively transfer the interfacial bond shear stress to the concrete surface through the adhesive layer, resulting in “ideal and reliable” interfacial stripping damage. Some specimens exhibited partial stripping and fracture of the CFRP sheet, potentially due to uneven stress from manual errors during bonding. And some CFRP sheets were fractured, primarily under high strain rates and when using longer bond lengths.

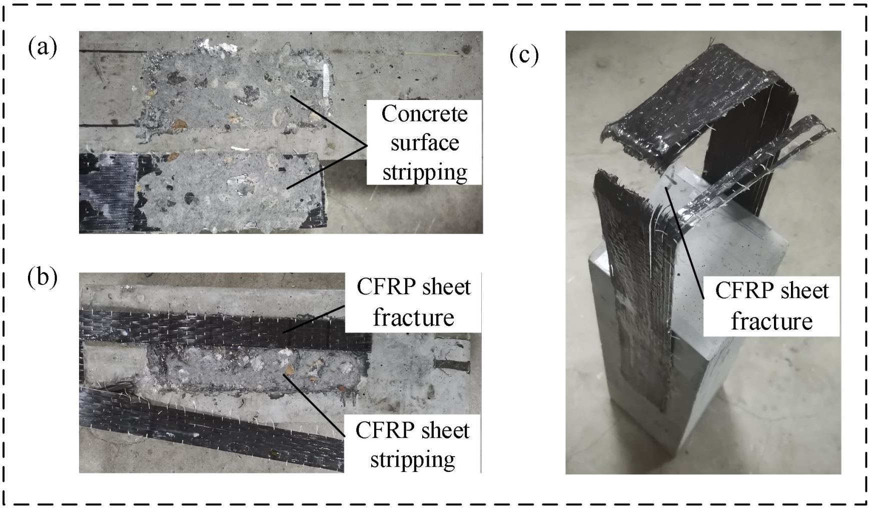

Fig. 2 Damage patterns: (a) debonding in concrete; (b) concrete debonding and partial CFRP sheet fractured; (c) CFRP sheet fractured.

Fig. 3 shows the stripping interface of some specimens. It can be seen that the surface layer of the peeled concrete contains broken recycled aggregates. This indicates that the aggregate is damaged during the failure process. Given that the strength of recycled aggregate is inferior to that of ordinary coarse aggregate, it can be reasonably assumed that the strength of the aggregate will impact the strength of the CFRP sheet-recycled aggregate concrete interface. This assertion is supported by the findings of previous studies, as cited in references [9]. This may result in a reduction in the strength at that interface between the CFRP sheet and the recycled aggregate concrete.

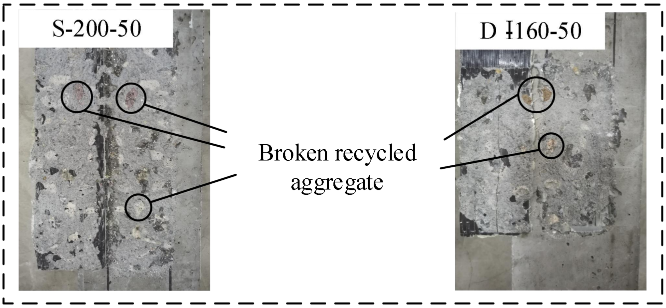

Fig. 3 Detailed view of the stripping interface.

3.2 Ultimate bearing capacity

The ultimate bearing capacity of concrete specimens with different bond lengths and different bond widths at different loading rates is given in Fig. 4. As shown in Fig. 4(a), the ultimate bearing capacity of the specimens at identical bond lengths demonstrates a progressive increase with the rise in loading rate. This indicates the existence of strain rate effect at the CFRP sheet-recycled aggregate concrete interface. The influence of load rate on ultimate bearing capacity decreases as the bond length increases. As an illustration, an increase in the loading rate from 0.1mm/min to 100mm/min has been observed to result in a 46.9%, 35.0%, and 27.4% enhancement in the ultimate bearing capacity, respectively, when the bond length was set at 40mm, 100mm, and 200mm. The ultimate bearing capacity of the specimen is observed to increase in accordance with the bond length, when the loading rate remains constant. Once the bond length reaches a specific value, the ultimate bearing capacity reaches a point of stability and begins to exhibit no further increase with the extension of CFRP bond length.

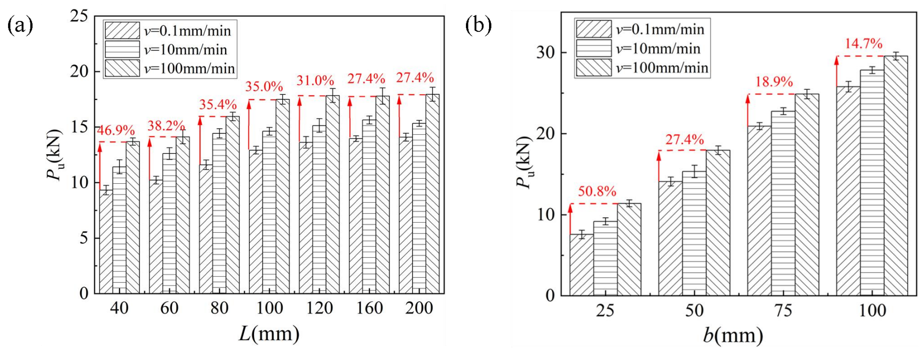

Fig. 4 Ultimate bearing capacity at different loading rates: (a) different bond lengths; (b) different bond widths.

From Fig. 4(b), it can be found that there is a notable enhancement in the ultimate bearing capacity of the specimens with an increase in the bond width. At a consistent loading rate, the bond width is essentially proportional to the ultimate bearing capacity. It can be observed that, when the bond width remains constant, an increase in loading rate results in a corresponding increase in the ultimate bearing capacity. The effect of the load rate on the ultimate bearing capacity is observed to diminish with an increase in the bond width. For example, an increase in the loading rate from 0.1 mm/min to 100 mm/min has been observed to result in a 50.8% enhancement in the ultimate bearing capacity when the bond width is 25 mm. When the bonding width is 100 mm, the ultimate bearing capacity exhibits a mere 14.7% increase.

3.3 Interfacial fracture energy

The interfacial fracture energy (G_f) is defined as the area enclosed by the stress-slip curve of the interface. It determines the magnitude of the interfacial bearing capacity and is the most important parameter in the stress-slip relationship. The study [10] showed that the bearing capacity of the CFRP-concrete interface is proportional to the square root of G_f, and has nothing to do with the specific form of stress-slip curve. The G_f of the specimen can be calculated by the following relation [10]:

$$G_{\mathrm{f}} = \frac{P_{\mathrm{u}}^2}{2b_{\mathrm{f}}^2 E_{\mathrm{f}} t_{\mathrm{f}}} \tag{1}$$

where, P_u represents the ultimate carrying capacity, b_f and t_f represent the width and nominal thickness of CFRP sheets, respectively, and E_f represents the elastic modulus of CFRP sheets.

Fig. 5 shows the impact of strain rate on G_f under different bond length and bond width. As illustrated in Fig. 5(a), an increase in the strain rate is observed to result in a corresponding rise in G_f at varying bond lengths. The G_f curves under different bond lengths are almost parallel. This shows that variations in bond length exert an influence solely on the specific value of G_f, without affecting its growth rate in response to an increase in the strain rate. Fig. 5(b) illustrates the impact of CFRP sheet bond width on G_f. The G_f of concrete specimens with small bond width is greater than that of concrete specimens with large bond width. For the specimen with small bonding width, G_f increases more obviously with increasing strain rate. This shows that when the bond width of CFRP sheet is small, the interface between CFRP sheet and recycled aggregate concrete has a more significant strain rate effect.

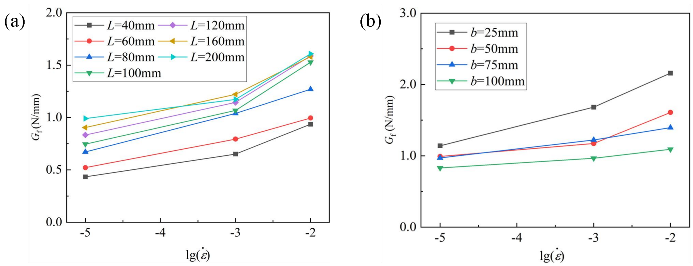

Fig.5 Influence of CFRP sheet on interfacial fracture energy: (a) different bond lengths; (b) different bond widths.

3.4 Local bond stress-slip relationships

The equations for calculating the interfacial shear stress and slip are as follows [11]:

$$\tau_i = \frac{\varepsilon_i - \varepsilon_{i+1}}{\Delta d} E_f t_f \ (i = 1 \sim n) \quad (2)$$

$$s_i = \frac{\varepsilon_i + \varepsilon_{i+1}}{2} \Delta d + \varepsilon_{i+1} \Delta d + s_{i+1} \ (i = 1 \sim n) \quad (3)$$

where ε_i represents the CFRP strain at Section i; ε_{i+1} represents the CFRP strain at Section i+1; s_i and s_{i+1} represent the slip of strain measurement points i and i+1; and Δd represents the interval between strain gauges (30 mm).

Fig. 6 illustrates the local stress-slip relationships under varying conditions. The stress-slip curve shows a consistent shape, with obvious rising and falling sections. Fig. 6(a) shows effect of bond length on the local stress-slip curve at a loading rate of 10 mm/min. It can be seen that the slopes of different curves are basically the same in the ascending and descending segments. The peak shear stress increases with the increase of the bonding length. Fig. 6(b) shows the stress-slip curves for different bond widths at the same loading rate. As the bond width decreases, the area encompassed by the interfacial bond stress-slip curve increases, which is consistent with the observed change in G_f. As the bond width increases, the peak shear stress and its corresponding slip decrease. In Fig. 6(c), the effect of loading rate on the local stress-slip curve is analyzed by taking the specimen with a bonding length of 200 mm and a bonding width of 50 mm as an example. It can be observed that the peak shear stress and the slip at the peak shear stress increase.

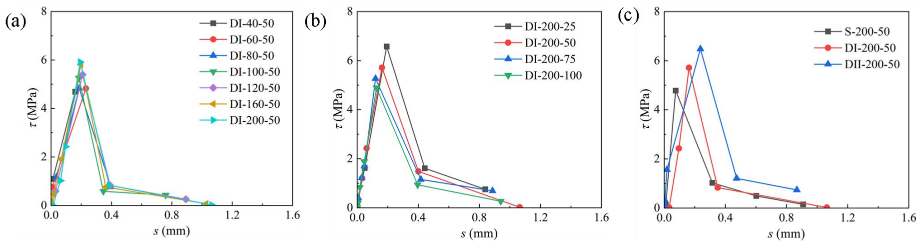

Fig.6 Local bond stress-slip relationships curve: (a) different bond lengths; (b) different bond widths; (c) different strain rates.

4 Conclusion

In this study, the dynamic interfacial bonding properties of CFRP sheet-recycled aggregate concrete under double-sided shear test were studied. The tests were conducted at varying loading rates to evaluate the impact of loading rate on the interfacial bonding properties of the concrete. Some concluding remarks are as follows.

1) The main damage pattern of the CFRP sheet-recycled aggregate concrete interface is the stripping damage of the concrete surface.

2) The ultimate bearing capacity of the CFRP sheet-recycled aggregate concrete interface showed an increasing trend with both bond length and bond width. The impact of load rate on ultimate bearing capacity is observed to diminish with the augmentation of bond length and bond width.

3) An increase in strain rate and bond length has been observed to result in an increase in interfacial fracture energy and interfacial shear stress, while a decrease is evident with an increase in bond width. The slip corresponding to the peak shear stress demonstrates a decrease with an increase in bond width and an increase with an increase in loading rate. The bond length has no discernible impact on the slip.

References

1. Xiao, J., Li, J., Lan, Y.: Research on recycled aggregate concrete-a review. Concrete, 17-20 (2003).
2. Naser, M.Z., Hawileh, R.A., Abdalla J.A.: Fiber-reinforced polymer composites in strengthening reinforced concrete structures: A critical review. Engineering Structures, 198, 109542 (2019).
3. Wang, B., Yan, L., Fu, Q., et al.: A Comprehensive Review on Recycled Aggregate and Recycled Aggregate Concrete. Resources. Conservation and Recycling, 171, 105565 (2021).
4. Mansour, W., Li, W., Wang, P., et al.: Experimental and numerical evaluations of the shear performance of recycled aggregate RC beams strengthened using CFRP sheets. Engineering Structures, 301, 117368 (2024).
5. Lawrence, C. B., Ardavan, Y., Ali, H., et al.: FRP strengthening of beams made with recycled concrete aggregate. ACI Special Publication, 322 (2018).
6. Tam, V.W.Y., Gao, X.F., Tam, C.M.: Microstructural analysis of recycled aggregate concrete produced from two-stage mixing approach. Cement and Concrete Research, 35(6), 1195-1203 (2005).
7. JGJ55-2011, Specification for mix proportion design of ordinary concrete. China Architecture & Building Press, Beijing (2011).
8. GB/T 3354-2014, Test method for tensile properties of orientation fiber reinforced polymer matrix composite materials. Standards Press of China, Beijing (2014).
9. Guo, H., Shi, C., Guan X., et al.: Durability of recycled aggregate concrete-A review. Cement and concrete composites, 89, 251-259 (2018).
10. Shi, J., Zhu, H., Wu, Z., et al.: Experimental study of the strain rate effect of FRP sheet-concrete interface. China Civil Engineering Journal, 45(12), 99-107 (2012).
11. Zhang, P., Gao, D., Zhu, H.: Numerical simulation and experimental study on the performance of wet-bonding interface between FRP plate and concrete. China Civil Engineering Journal, 46(2), 108-114 (2013).